

# EXPERIMENTAL STUDY OF THE FLAME INHIBITION EFFECT OF IRON PENTACARBONYL

Dirk Reinelt and Gregory T. Linteris

National Institute of Standards and Technology,  
Gaithersburg MD 20899, USA

## INTRODUCTION AND BACKGROUND

The ban on the production of the fire suppressant  $CF_3Br$  has created a need for replacement agents. Obvious alternatives are other halogenated hydrocarbons, and much research has recently been devoted to understanding their relative performance and inhibition mechanisms [1-6]. However, an agent with all of the desirable properties of  $CF_3Br$  is proving difficult to find. Consequently, the National Institute of Standards and Technology (NIST) is undertaking research to identify new chemical suppressants and understand the mechanisms of inhibition of known agents, particularly those which have shown strong inhibiting effects.

In the 1960s, Lask and Wagner [7] performed a comprehensive study of the flame inhibiting effects of a wide range of compounds, and determined that organometallic compounds are powerful flame inhibitors. One of the most effective was iron pentacarbonyl  $Fe(CO)_5$ , a highly flammable, viscous liquid (melting point  $-20\text{ }^\circ\text{C}$ ; boiling point  $103\text{ }^\circ\text{C}$ ; vapor pressure about  $2900\text{ N/m}^2$  at  $20\text{ }^\circ\text{C}$  [8]). It was found to be several orders of magnitude more effective than the halogens at reducing the burning rate of premixed hydrocarbon-air flames. Wagner and coworkers attempted, in continuing research [9, 10], to understand iron pentacarbonyl's behavior through spectroscopic measurements in low-pressure flames, but the work was discontinued (presumably due to the rapid adoption of  $CF_3Br$ ). Consequently, the mechanism of inhibition of  $Fe(CO)_5$  remains undetermined for premixed flames, and the agent has not been systematically tested in diffusion flames, which are more representative of fires. Although one would never use iron pentacarbonyl to extinguish fires in occupied spaces because of its high toxicity, it is *so* efficient that an understanding of its inhibition mechanism may provide possible avenues for developing new inhibitors.

Iron pentacarbonyl forms condensed-phase particulates [7] upon passing through a flame, and it is unresolved whether its inhibition mechanism is due to gas-phase or heterogeneous effects [9]. Interestingly, other very effective inhibitors also involve a condensed phase. These include agents which form the particulates after passing through the flame; i.e., flame generated particulates, as well as agents which are initially added as a condensed phase. The former category includes other organometallics compounds such as lead tetraethyl and nickel carbonyl and the halometallic compounds  $TiCl_4$

and  $SnCl_4$  [7]. A new class of fire suppressants, pyrotechnically generated aerosols [11], may work similarly, since these generate particulates through solid-propellant reactions in a flame separate from the fire to be extinguished. It is possible that part of the effectiveness of these agents is due to the action of either gas- or condensed-phase metal and metal oxide compounds. The latter category, powders, includes the widely used alkali salt powders  $NaHCO_3$  and  $KHCO_3$  [12] and other metal salts [13] which can be several times more effective than  $CF_3Br$ . Finally, this latter category also includes a new type of suppressant, non-volatile organic precursors [14] which decompose near the flame to release species with strong inhibiting action.

These condensed-phase agents have many similarities, in particular, their strong inhibiting action and the lack of a complete understanding of their modes of inhibition. For example, the relative importance of physical, thermal, and chemical effects have not been clearly discerned for any of the agents, nor have the roles of heterogeneous versus homogeneous chemistry. Also, many studies in the past screened a large number of compounds rather than investigating one compound in detail. The approach in this research is to select one condensed-phase inhibitor and study its action, both experimentally and numerically. Many of the experimental and analytical tools developed will then be applicable to other heterogeneous inhibitors. Because  $Fe(CO)_5$  is so effective, it was selected first for further study.

The approach in the present research is to use simple laboratory burners, both premixed Bunsen-type flames and counterflow diffusion flames, to obtain global, yet fundamental information on the action of iron pentacarbonyl. The burning velocity and extinction strain rate, both of which provide a measure of the overall reaction rate, are determined with addition of iron pentacarbonyl, while varying the stoichiometry, oxygen mole fraction, flame temperature, and flame location.

The present results supplement previously reported tests on methane and propane premixed flames with argon as the carrier gas for the  $Fe(CO)_5$  [15]. By using nitrogen as the carrier gas, the present experiments eliminate the complications arising from a lowered temperature due to argon dilution, and permit experiments at variable oxygen mole fraction. Extension of the experiments to counterflow diffusion flames allows control of the chemical environment, the location where the metal-containing species are formed, and the transport of these species to the reaction zone. Ultimately, the research will include detailed numerical calculations including full chemistry, transport, and particulate growth, chemistry, and dynamics. The present paper describes preliminary experimental results. It consists of two major parts describing premixed flames and counterflow diffusion flames separately.

## PREMIXED FLAMES

### Experimental Apparatus and Procedure

The decrease in the laminar burning velocity is used in the present work as a measure of the inhibition action of iron pentacarbonyl. For the premixed flame burning velocity measurements, a 1.02 cm diameter nozzle burner [16] produces a 1.3 cm tall Bunsen flame (Fig.1). The burner is placed in a square acrylic chimney with no co-flowing gases. The experimental system has been described previously [17]. In the present work, however, the flame height is held constant and no schlieren images are taken of the flame. Since the burner produces schlieren and visible images which are very nearly straight-sided and parallel, the flame area has been found to remain within a few percent if the flame height is held constant (even as the burning velocity is reduced by 60%).

Fuel, oxygen, nitrogen, and  $Fe(CO)_5$  carrier gas flows are measured with digitally-controlled mass flow controllers (Sierra Model 860\*) with a claimed precision of 0.2% and accuracy of 1%, which have been calibrated with bubble and dry (American Meter Co. DTM-200A) flow meters so that their accuracy is 1%. The fuel gas is methane (Matheson, 99.97%), and the oxidizer stream consists of nitrogen (boil-off from liquid nitrogen) and oxygen (Potomac Air Gas, 99.8%). All gases pass through heat exchangers prior to entering the burner to maintain them at the laboratory temperature of 23°C. Part of the nitrogen stream is diverted, and bubbles through the liquid  $Fe(CO)_5$  (Aldrich) in a two-stage saturator in an ice bath. This carrier flow (always less than 0.4 l/min) is assumed to be saturated. The gas-flow lines which are located after the saturator but before the point of dilution by the bulk of the gas flow are maintained at 39°C to avoid condensation of the  $Fe(CO)_5$ .

For these experiments, the inhibitor concentration in the premixed gases is increased and the total flow reduced as necessary to maintain the desired flame height. Software control of the gas flows allows reduction in the total flow while maintaining constant values of the stoichiometry, and oxygen and  $Fe(CO)_5$  mole fractions. The average burning rate for the flame is determined using the total area method assuming a constant value for the flame area. Although measurement of a true one-dimensional, planar, adiabatic burning rate is difficult [18], the relative change in the burning rate can be measured with more confidence. Consequently, the burning rate reduction in the present work is normalized by the uninhibited burning rate.

---

\*Certain trade names and company products are mentioned in the text or identified in an illustration in order to specify adequately the experimental procedure and equipment used. In no case does such identification imply recommendation or endorsement by the National Institute of Standards and Technology, nor does it imply that the products are necessarily the best available for the purpose.

## Results and Discussion

The uninhibited premixed flame is blue. Addition of 10 ppm of  $Fe(CO)_5$  turns the flame orange, and the intensity increases with increasing  $Fe(CO)_5$  mole fraction. The orange emission is uniformly bright in the post combustion region for about 1 cm downstream, and the intensity appears greatest in the reaction zone of the flame.

The normalized burning velocity of the premixed methane-air flame inhibited by iron pentacarbonyl is shown in Fig. 2 for a fuel/air equivalence ratio  $\phi$  of 0.9, 1.0, and 1.1. The stoichiometric and rich flames are affected about equally by the  $Fe(CO)_5$ , while the lean flame shows twice as much reduction in the burning velocity at low  $Fe(CO)_5$  concentrations, and could not be stabilized above 41 ppm, where the burning rate reduction is 30%. Most notable, above about **200** ppm, there does not appear to be any additional inhibition effect of the iron pentacarbonyl for the stoichiometric and rich flames.

Table 1 lists the equivalence ratio and oxygen mole fractions for the flames presented in Fig. 2, as well as the experimentally measured burning velocities of the uninhibited flames, and the slope of the inhibitory effect at zero iron pentacarbonyl mole fraction. This slope is expressed as the inhibition index suggested by Fristrom and Sawyer [19],  $\Phi_0 = -\frac{dV_i}{dX_i} \frac{X_{O_2}}{V_i}$ , where  $V_i$  and  $\frac{dV_i}{dX_i}$  are the burning velocity and slope of the burning velocity reduction with inhibitor addition at zero inhibitor, and  $X_{O_2}$  is the oxygen mole fraction. The inhibition index  $\Phi_0$  for iron pentacarbonyl is seen to range from 850 to 1650; as Fig. 2 shows, the index goes to zero above 300 ppm. The value of  $\Phi_0$  for  $CF_3Br$ , which shows little variation with  $CF_3Br$  mole fraction, is only about 20 [20]. For the agents  $CF_3H$ ,  $C_2HF_5$ , and  $C_3HF_7$ , this index, representing the initial inhibitory effect in stoichiometric premixed methane-air flames, is **3.3**, 3.9 and 6.9 [17, 21]. These numbers show the superior effectiveness of  $Fe(CO)_5$  as an inhibitor.

The mechanism of the inhibiting action of iron pentacarbonyl is still unknown. The results are consistent with an inhibition mechanism involving catalytic recombination of H-atoms by an iron compound, as explained in ref. [22], but more research is necessary in this area.

The data in this paper supplement the findings of Wagner et al. [7, 9, 10]. Although the inability of iron pentacarbonyl to reduce the burning rate of premixed methane-air flames beyond a factor of two may at first be thought to be disappointing, it does not necessarily eliminate such a compound from use. For example, since only minute quantities are required to obtain such a strong effect, an iron compound might be added to some other agent, the combination of which reduces the burning velocity sufficiently far.

## COUNTERFLOW DIFFUSION FLAMES

While co-flow diffusion flame burners such as the cup burner have been very useful for agent screening, they are not amenable to detailed modeling and subsequent interpretation of the mechanism of inhibition of an agent. In the cup burner, the flame is believed to be stabilized by a region at the burner rim where premixing of the fuel and oxidizer occurs. Inhibitor added to the oxidizer stream is transported by diffusion or convection to the stabilization region, and slows the overall reaction rate causing flame blow-off and extinction. Because of the complex aerodynamics in the stabilization region, it is difficult to know the flux of agent into this premixed region, and hence to interpret the inhibition mechanism. A counterflow configuration provides a diffusion flame with a more readily interpreted extinction condition. The flow field is easy to describe mathematically and the governing equations can be reduced to one-dimensional form, greatly facilitating numerical calculations. The burner does not have the premixed region at the base, and the flux rates of fuel, oxidizer, and agent to the reaction zone are easily calculated.

In a counterflow diffusion flame (Fig. 3), the fuel and oxidizer streams flow towards each other in stagnation flow about the stagnation plane. The flame is established at the point where the fuel and oxidizer are convected or diffuse together in stoichiometric proportions. This location depends upon the relative moles of fuel and oxygen necessary for stoichiometric reaction, the mole fraction of fuel and oxygen in the two streams, and the relative diffusion rates of the fuel and oxygen. By diluting either stream, the flame can be established on either side of the stagnation plane. The fuel and oxidizer streams of a diffusion flame have different chemical environments, the former a reducing environment and the latter, an oxidizing. Hence, by varying the flame location, diluent concentrations, and location of iron pentacarbonyl injection, the chemical environment, temperature, and transport of inhibiting species to the reaction zone can be controlled. The four cases of flame and inhibitor location are depicted in Fig. 3.

### Experimental Apparatus and Procedure

The burner used for the counterflow experiments is described in detail in ref. [23]. It consists of two opposing ducts of 22.2 mm inner diameter which are 11 mm apart. A number of fine wire screens (60 mesh/cm) are placed in each duct to produce laminar flow. Annularly co-flowing nitrogen around the lower duct shields the flame from the ambient air and prevents after-burning of the gases in the exhaust. A water-cooled heat exchanger surrounds the upper duct and mild suction withdraws the combustion products. Because of the high toxicity of iron pentacarbonyl, mild suction is also employed outside the heat exchanger and the experiment is operated in a chemical hood.

The fuel, air, and carrier gas flows are measured with digitally-controlled mass flow

controllers described above. The fuel gas methane (Matheson, 99.97%) flows from the top duct, while the oxidizer gas, produced by mixing nitrogen (boil-off) and oxygen (Potomac Air Gas, 99.8%), flows from the bottom. Air could not be used as the carrier gas for the inhibitor due to the reaction of  $O_2$  with  $Fe(CO)_5$  and subsequent particulate formation in the bubbler. Therefore, the iron pentacarbonyl is added to the fuel or the oxidizer stream by bubbling methane or nitrogen through a two-stage saturator in a water bath at a controlled temperature of 17-22 °C. The gas-flow lines which are located after the saturator but before the point of dilution by the bulk of the gas flow are maintained at 39 °C to avoid condensation of the  $Fe(CO)_5$ . All experiments were performed at ambient pressure and with the gas flows at ambient temperature

The reduction in the extinction strain rate is used as a measure of the inhibition action of iron pentacarbonyl. To run an experiment, a diffusion flame is first established at a predetermined condition of a low strain rate. The strain rate, seen as the maximum value of the oxidizer-side velocity gradient just prior to the flame, can be approximated from the outer flow jet exit velocities according to  $a_0 = \frac{2|v_0|}{L} \left(1 + \frac{|v_F| \sqrt{\rho_F}}{|v_0| \sqrt{\rho_0}}\right)$  [24]. Here  $L$  denotes the distance between the ducts,  $v$  the velocity,  $\rho$  the density and the subscripts  $F$  and  $0$  the fuel and oxidizer stream, respectively. The jet exit velocities are chosen so that the momentum of the two streams is balanced at all values of the strain rate; i.e.,  $\rho_F v_F^2 = \rho_0 v_0^2$ . Doing so ensures that the flame, which is usually close to the stagnation plane, is kept away from the exits of the two gas streams and is found to be approximately in the middle of the ducts. Inserting the momentum balance into the equation for the strain rate gives  $a_0 = \frac{4|v_0|}{L}$ . If the flame sits on the fuel side of the stagnation plane the equations have to be changed appropriately, leading to  $a_F = \sqrt{\frac{\rho_0}{\rho_F}} a_0$ , where  $a_F$  is the strain rate (i.e., velocity gradient) on the fuel side. When a flame is stabilized the agent is added and the value of the strain rate is gradually increased by proportionately increasing all flows. When the critical value of the strain rate is reached the flame extinguishes abruptly; this value is recorded as the extinction strain rate which is found with an uncertainty of  $\pm 5\%$ .

## Results and Discussion

Depending on the dilution of the fuel and the oxidizer stream, the flame will be located on either the fuel or the oxidizer side of the stagnation plane. Additionally, the inhibitor can be added to either the fuel or the oxidizer stream. Hence the inhibitor may be transported to the reaction zone either by convection (fast) or diffusion (slower) after having interacted with an oxidizing or reducing environment. Results for each case are discussed below.

Figure 4 shows the extinction strain rate versus the molar concentration (in ppm) of inhibitor ( $Fe(CO)_5$ ) for the case of undiluted air versus undiluted methane (where the flame is located on the oxidizer side of the stagnation plane). Adding iron pen-

tacarbonyl to the oxidizer stream decreases the extinction strain rate rapidly for mole fractions up to 80 ppm. Above this value, the extinction strain rate decreases less rapidly but roughly in proportion to the increase in  $Fe(CO)_5$ . Nevertheless, up to the amount of inhibitor used in the experiment (which was limited by the saturator), the incremental inhibiting effect of  $Fe(CO)_5$  does not become zero as in the premixed flame.

The inhibition effect of  $Fe(CO)_5$  added to the air stream of a counterflow diffusion flame is much stronger than that of  $CF_3Br$ : an  $Fe(CO)_5$  mole fraction of 500 ppm reduces the extinction strain rate by about 30% whereas 6000-7500 ppm of  $CF_3Br$  and about 20 000 ppm of  $CF_3H$  are necessary for an equivalent reduction [25, 26]. When the iron pentacarbonyl is added to the oxidizer, the originally blue flame changes to very luminous, bright orange, likely due to the formation of  $FeO$  which has strong emission at 591 nm [9]. A deposition of red/orange particles, presumably iron oxides, is observed in the exhaust system after the experiments.

On the contrary, Fig. 4 shows that adding  $Fe(CO)_5$  to the fuel stream increases the extinction strain rate. Iron pentacarbonyl no longer acts as an inhibitor in this case, but rather promotes the combustion. The increase in the extinction strain rate is small compared to the magnitude of the decrease from addition to the oxidizer stream but it is clearly noticeable. This flame does not change its color but remains blue. The reason for this increase is unclear. Since thermal decomposition of  $1Fe(CO)_5$  may produce  $5CO$ , tests were conducted to examine the effect of 1000 ppm of  $CO$  in the fuel stream when no inhibitor was present. However, these experiments showed no effect from the added  $CO$ .

Contrasting results were obtained with an oxidizer stream of 45%  $O_2/55\% N_2$  (all values given as molar concentrations) and a fuel stream of 13%  $CH_4/87\% N_2$  (which puts the flame on the fuel side of the stagnation plane). Figure 5 shows the effect of adding  $Fe(CO)_5$  to oxidizer and fuel stream, respectively. In both cases, the strain rate at extinction decreases slightly, a few percent at an inhibitor mole fraction of 80 ppm, above which there is no additional effect. Overall, the inhibiting effect of adding iron pentacarbonyl to that flame is almost negligible. For the addition of  $Fe(CO)_5$  to the fuel or the oxidizer stream, a red layer formed on the side of the blue flame facing the iron pentacarbonyl injection,

An important influence is obviously the availability of oxygen for the inhibitor prior to the flame, and possibly different transport rates of the inhibiting species to the reaction zone. It can be seen that the strong inhibiting effect is performed only if the flame is on the oxidizer side and the inhibitor is added to the oxidizer stream.

The reasons for the inhibiting and promoting behavior of  $Fe(CO)_5$  in the counterflow flames described above are still unclear. The present data showing inhibition are consistent with both the homogeneous and heterogeneous mechanisms of catalytic

recombination of radicals. A homogeneous catalytic cycle involving the recombination of H-radicals and also the same mechanism running in reverse direction, i.e., producing H-radicals [22], could be responsible for the observed behavior. Since the condensed-phase species are probably iron oxides, and oxygen is needed for their formation, most of the above observations are also consistent with a heterogeneous catalytic mechanism. Finally, the reduced effect of iron pentacarbonyl at higher concentrations in the diffusion and premixed flame can be rationalized with either homo- or heterogeneous mechanisms. Above a certain iron mole fraction in the flame, the gas-phase catalytic iron-intermediate may no longer be the deficient reactant. Conversely, if it is a surface effect, above a certain iron loading in the flame, the particles may agglomerate faster than new particles are formed, leading to no increase in the total surface area for inhibition.

The present experimental results elucidate many details of the inhibition by  $Fe(CO)_5$  but they do not reveal its precise mechanism. Particle measurements are planned to learn more about the homogeneous or heterogeneous reaction mechanism.

## SUMMARY

The inhibiting action of iron pentacarbonyl on the burning velocity and extinction strain rate of premixed and diffusion flames of methane, oxygen, and nitrogen has been examined systematically. In premixed flames, behavior at low and high iron pentacarbonyl mole fractions is distinctly different: the reduction in burning velocity is very strong for an inhibitor mole fraction up to about 100 ppm, above which there is negligible additional inhibition. In counterflow diffusion flames with the flame on the oxidizer side of the stagnation plane and iron pentacarbonyl added to the oxidizer stream, the inhibitory effect is also very strong. The rate of decrease in extinction strain rate is greatest for iron pentacarbonyl mole fractions below 100 ppm; however, in contrast to the premixed flames, the inhibition effect continues even above 500 ppm. Interestingly, when  $Fe(CO)_5$  is added to the fuel stream in the diffusion flame, there is an apparent promotion of the combustion. Finally, when the flame is located on the fuel side, there is a negligible effect of  $Fe(CO)_5$  when it is added to either stream. These results appear to be consistent with an inhibition mechanism involving catalytic recombination of  $H$  radicals; homogeneous or heterogeneous reactions might be responsible. Additional research is under way in order to understand the observed behavior.

## ACKNOWLEDGMENTS

The financial support of the Alexander von Humboldt Foundation for one of the authors (DR) is gratefully acknowledged. The authors thank Newton and Arnold Liu for assisting with the software development and the premixed flame experiments. Helpful conversations with D. Trees greatly facilitated the diffusion flame experiments.



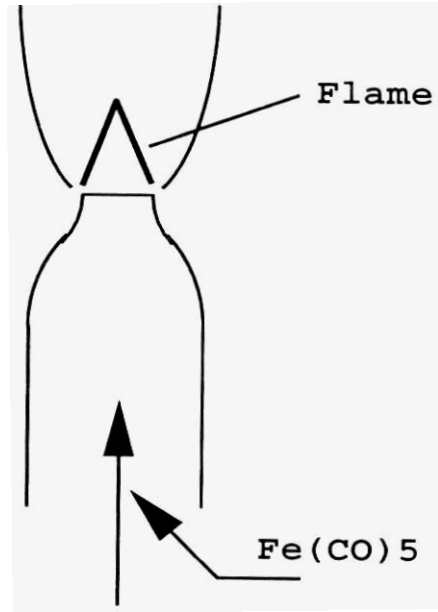
## REFERENCES

- [1] Burgess, D.R.F., Jr., Zachariah, M.R., Tsang, W., and Westmoreland, P.R., *Halon Replacements: Technology and Science*, A.C.S. Symposium Series (A.W. Miziolek, and W. Tsang, Eds.), Washington D.C., 1995, pp. 322-340.
- [2] Gann, R.G. (Ed.), National Institute of Standards and Technology, Gaithersburg MD, NIST SP 890, 1995.
- [3] Sheinson, R.S., Penner-Hahn, J.E., and Indritz, D., *Fire Safety Journal* 15: 437-450, 1989.
- [4] Battin-Leclerc, F., Walravens, B., Côme, G.M., Baronnet, F., Sanogo, O., Delfau, J.L., and Vovelle, C., *Halon Replacements: Technology and Science*, A.C.S. Symposium Series (A.W. Miziolek, and W. Tsang, Eds.), Washington D.C., 1995, pp. 289-303.
- [5] Richter, H., Rocteur, P., Vandooren, J., and Van Tiggelen, P.J., *Halon Replacements: Technology and Science*, A.C.S. Symposium Series (A.W. Miziolek, and W. Tsang, Eds.), Washington D.C., 1995, pp. 303-321.
- [6] Trees, D., Seshadri, K., and Hamins, A., *Halon Replacements: Technology and Science*, A.C.S. Symposium Series (A.W. Miziolek, and W. Tsang, Eds.), Washington D.C., 1995, pp. 190-203.
- [7] Lask, G., and Wagner, H.G., *Eighth Symposium (International) on Combustion*, Williams and Wilkins Co., Baltimore, p. 432, 1962.
- [8] Gmelin Handbuch der Anorganischen Chemie, Nr. 59 Fe, Eisen-Organische Verbindungen, Teil B3, Springer, 1979.
- [9] Bonne, U., Jost, W., and Wagner, H.G., *Fire Research Abstracts and Reviews* 4: 6, 1962.
- [10] Jost, W., Bonne, U., and Wagner, H.G., *Chem. Eng. News* 39: 76, 1961.
- [11] Kimmel, E.C., Smith, E.A., Reboulet, J.E., Black, H.H., Sheinson, R.S., and Carpenter, R.L., *Halon Options Technical Working Conference*, Albuquerque, NM, May 9-11, 1995, p. 499-520.
- [12] Rosser, W.A., Inami, S.H., and Wise, H., *Combust. Flame* 7: 107, 1963.
- [13] Vanpee, M., and Shirodkar, P., *Seventeenth Symposium (International) on Combustion*, The Combustion Institute, Pittsburgh, p. 787, 1979.
- [14] Bannister, W.W., McCarthy, D.W., Watterson, A., Patronick, J., Floden, J.R., and Tetla, It., *Halon Options Technical Working Conference*, Albuquerque, NM, May 9-11, 1995, p. 357-367.
- [15] Linteris, G.T., and Gmurczyk, G., *15th International Colloquium on the Dynamics of Explosions and Reactive Systems*, July 31- August 4, 1995, Boulder, CO, pp. 298-301.
- [16] Mache, H., and Hebra, A., *Sitzungsber. Osterreich. Akad. Wiss., Abt. IIa*, 150: 157, 1941.
- [17] Linteris, G.T., and Truett, L.F., *Combust. Flame* 105: 15-27, 1996.
- [18] Andrews, G.E., and Bradley, D., *Combust. Flame* 18: 133-153, 1972.

- [19] Fristrom, R.M., and Sawyer, R., *AGARD Conf. on Aircraft Fuels, Lubricants and Fire Safety*, AGARD-CP 84-71, 1971.
- [20] Rosser, W. A., Wise, H., and Miller, J., *Seventh Symposium (International) on Combustion*, Butterworths, London, 1959, pp. 175-182.
- [21] Linteris, G.T., Burgess, D.R., Babushok, V., Zachariah, V., Westmoreland, P., and Tsang, W., "Inhibition of Premixed Methane-Air Flames by Fluoroethanes and Fluoropropanes", to be submitted for publication in *Combust. Flame*, May 1996.
- [22] Reinelt, D., and Linteris, G.T., "Experimental Study of the Inhibition of Premixed and Diffusion Flames by Iron Pentacarbonyl", accepted for presentation at the *26th Symposium (Int.) on Combustion*, July 28 - August 2, 1996, Naples, Italy.
- [23] Puri, I.K., and Seshadri, K., *Combust. Flame* 65: 137-150, 1986.
- [24] Seshadri, K., and Williams, F.A., *Int. J. Heat Mass Transfer* 21: 251-253, 1978.
- [25] Milne, T.A., Green, C.L., and Benson, D.K., *Combust. Flame* 15: 255, 1970.
- [26] Trees, D., Grudno, A., Ilincic, N., Weißweiler, T., and Seshadri, K., *Proceedings of the Joint Technical Meeting*, The Central States/Western States/Mexican National Sections of the Combustion Institute, San Antonio, TX, April 23-26, 1995, pp. 227-232.

$\phi$	$X_{O_2}$	$V_{exp}$	$\Phi_0$
0.9	0.21	37.1	1648
1.0	0.21	40.6	850
1.1	0.21	<b>39.3</b>	845

**Table 1:** Equivalence ratio  $\phi$ , oxygen mole fraction  $X_{O_2}$ , measured burning velocity  $V_{exp}$  and inhibition index  $\Phi_0$  at zero inhibitor mole fraction. Data are presented for the experimental conditions of Fig. 2.



Premixed gases  
[CH<sub>4</sub>, O<sub>2</sub>, N<sub>2</sub>]

Figure 1: Premixed flame,

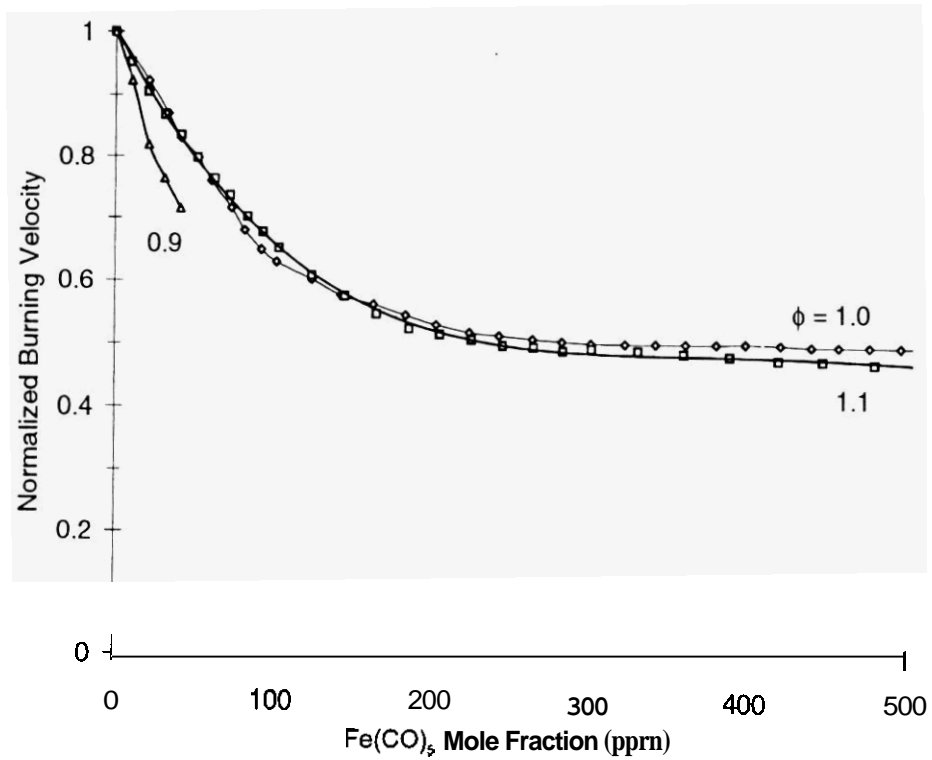
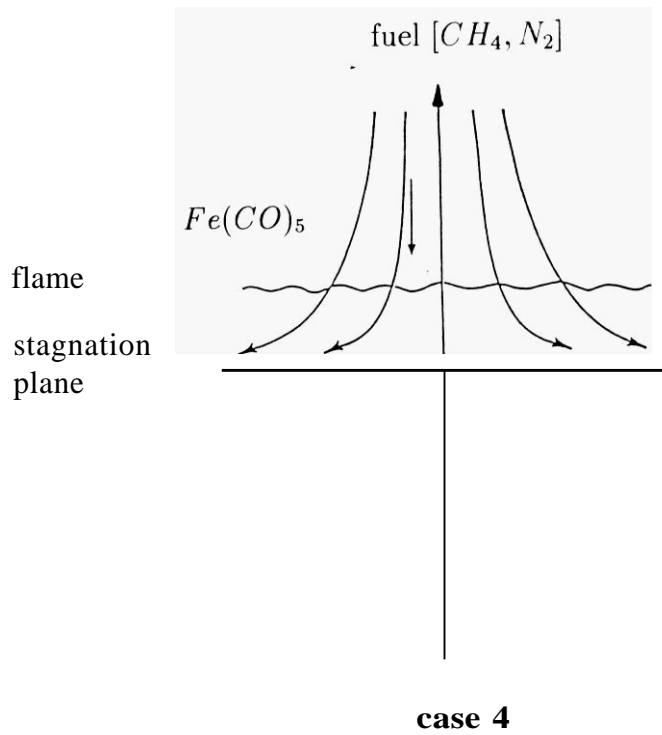
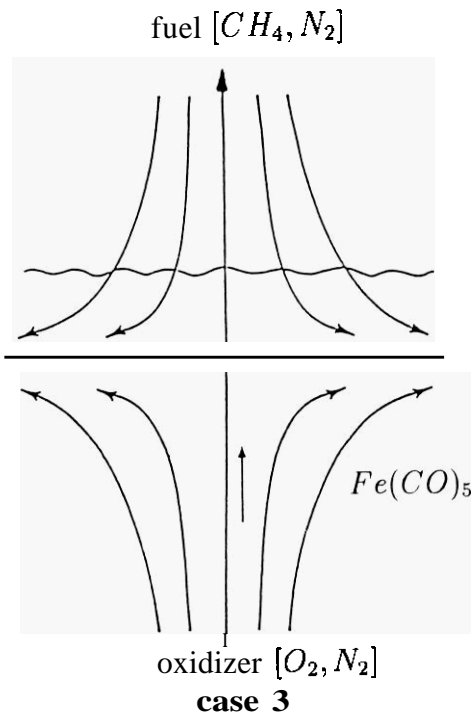
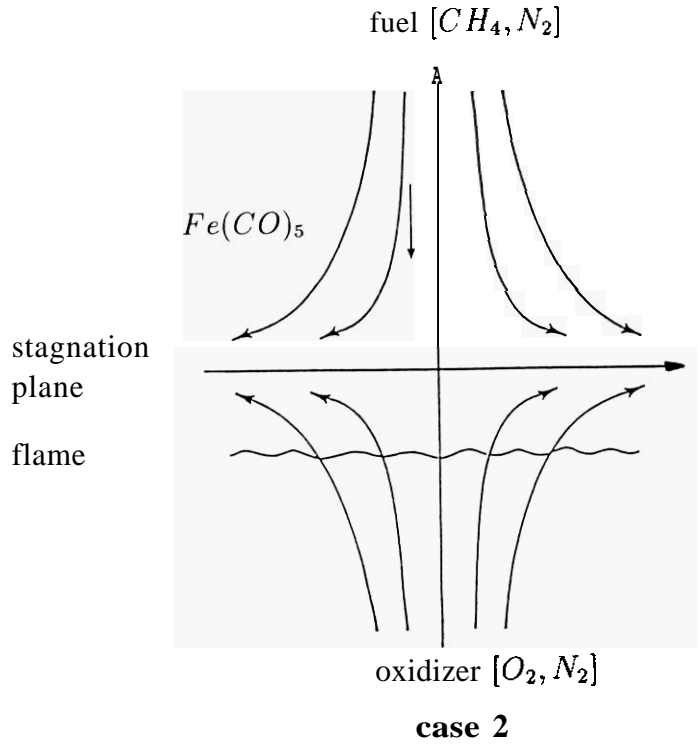
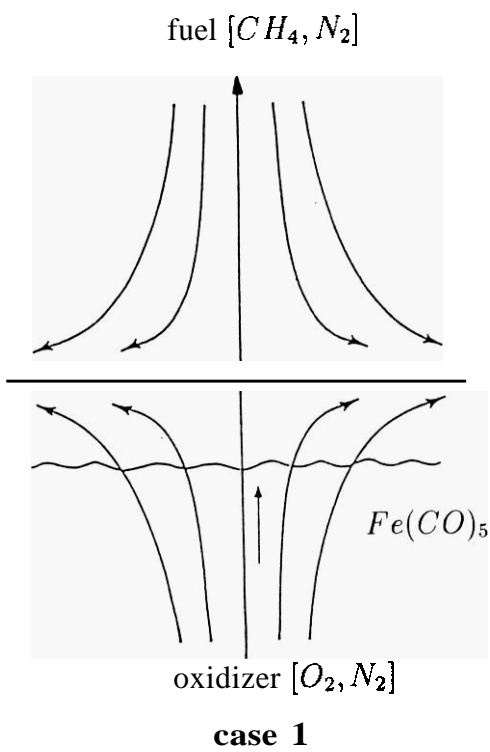
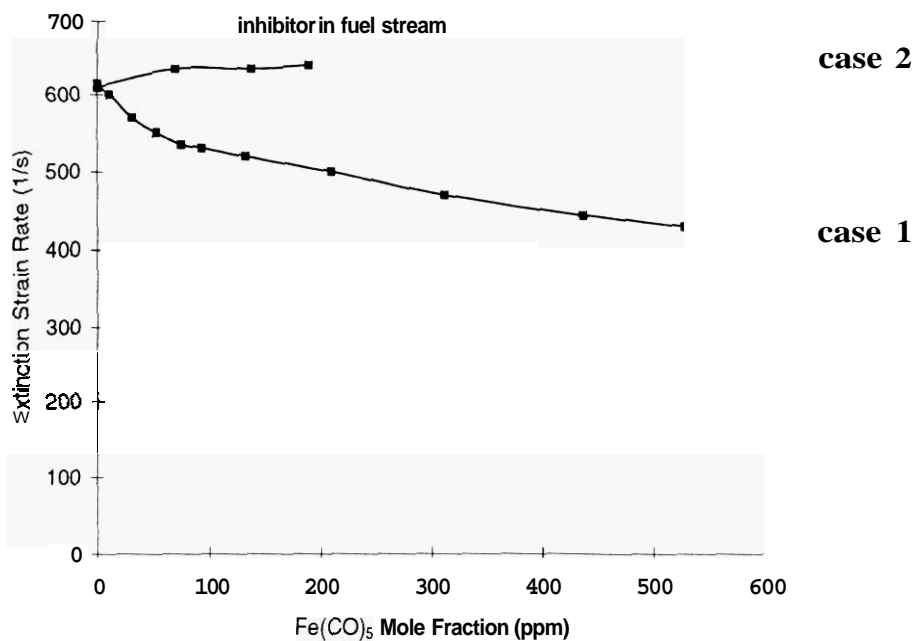


Figure 2: Premixed methane-air flame,  $X_{O_2}=0.21$ ,  $\phi=0.9, 1.0,$  and  $1.1.$



**Figure 3:** Cases studied for the counterflow diffusion flames



**Figure 4:** Counterflow diffusion flame; undiluted air versus undiluted methane (flame on oxidizer side).

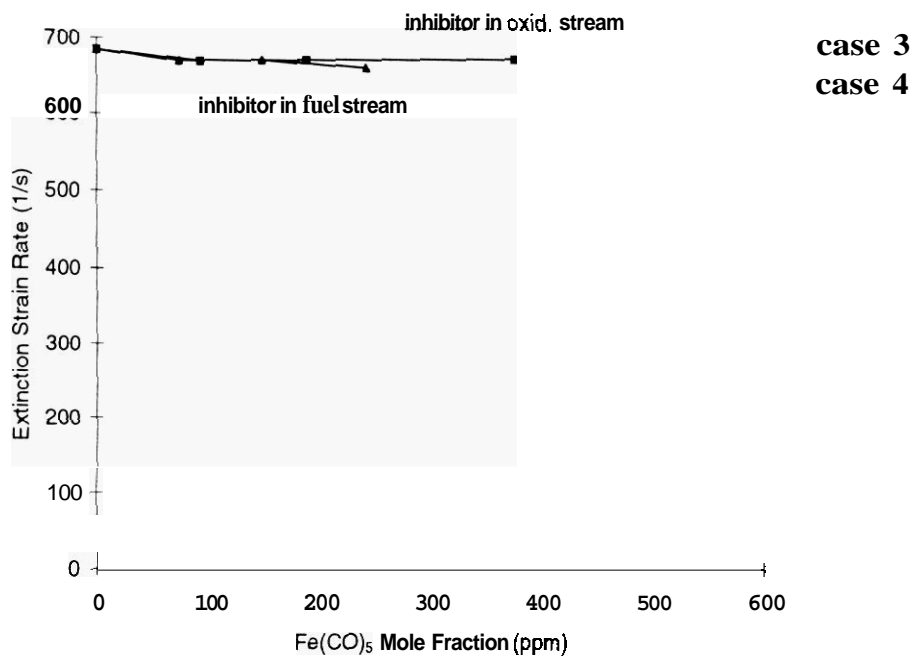


**Figure 5:** Counterflow diffusion flame; 45% O<sub>2</sub>/55% N<sub>2</sub> vs. 13% CH<sub>4</sub>/87% N<sub>2</sub> (flame on fuel side).

